MAUSAM, **74**, 2 (April, 2023), 267-272

MAUSAM

DOI : https://doi.org/10.54302/mausam.v74i2.5992
Homepage: https://mausamjournal.imd.gov.in/index.php/MAUSAM

UDC No. 551.553.21 : 551.555.1

Equatorial Rossby waves and their impacts on monsoon region deep convection

PAUL E. ROUNDY

State University of New York

Albany, NY, United States

e mail : proundy@albany.edu

सार – **संवहन युग्मित विषुवतीय रॉस्बी तरंगें उष्ण कटिबंध में पश्चिम की ओर बढ़ने वाले उप-मौसमी संवहन की प्रमुख प्रणाली हैं।इन तरंगों में विचरण के एक हिस्से को उष्णकटिबंधीय अंतरामौसमी दोलन के साथ संबद्ध करने के लिए दिखाया गया है, साथ ही उष्णकटिबंधीय संवहन के लिए अतिरिक्त उष्णकटिबंधीय रॉस्बी तरंग प्रतिक्रिया द्वारा मध्यस्थता वाली प्रक्रिया के साथ-साथ रॉस्बी तरंगों को उष्णकटिबंधीय वातावरण में कमजोर होने को दिखाया गया है।रॉस्बी वेव ब्रेकिंग द्वारा संचालित संभावित भ्रमिलता विसंगतियाँ भूमध्यरेखीय रॉस्बी तरंगें बन जाती हैं। यह कार्य ग्रहीय पैमाने के भूमध्यरेखीय रॉस्बी तरंगों का एक सूचकांक बनाता है और उष्णकटिबंधीय और अतिरिक्त उष्णकटिबंधीय परिसंचरण सुविधाओं के साथ अपने पसंदीदा संघों का निदान करने के लिए ऋतुनिष्ठ भिन्न प्रतिगमन ढलान गुणांक की विधि को लागू करता है। परिणाम इन तरंगों और अतिरिक्त उष्णकटिबंधीय वातावरण के बीच पहले से ही ज्ञात संबंध की पुष्टि करते हैं, और वे उत्तरी गोलार्ध की गर्मियों के दौरान हिंद महासागर और दक्षिणी एशिया में उष्णकटिबंधीय संवहन के पश्चिम और उत्तर की ओर बढ़ने वाली विसंगतियों का एक पैटर्न प्रकट करते हैं। ये पैटर्न संवहन के दमन और संवर्द्धन के एक चक्र से जुड़े हैं जिसमें बहिर्गामी दीर्घ तरंग विकिरण की नकारात्मक विसंगतियाँ लहरों के शुष्क दौरकी तुलना में गीले दौरके दौरान** 3 **गुना अधिक होने की संभावना पाई जाती हैं।**

ABSTRACT. Convectively coupled equatorial Rossby waves are the dominant mode of westward-moving subseasonal convection in the tropics. A portion of the variance in these waves has been shown to associate with the tropical intraseasonal oscillation, along with a process often mediated by the extratropical Rossby wave response to tropical convection that yields Rossby waves breaking back into the tropical atmosphere. The potential vorticity anomalies driven by Rossby wave breaking become the equatorial Rossby waves. This work creates an index of planetary scale equatorial Rossby waves and applies the method of seasonally varying regression slope coefficients to diagnose their preferred associations with tropical and extratropical circulation features. Results confirm the already known association between these waves and the extratropical atmosphere and they reveal a pattern of westward-and northward-moving anomalies of tropical convection over the Indian Ocean and Southern Asia during the Northern Hemisphere summer. These patterns are associated with a cycle of suppression and enhancement of convection in which negative anomalies of outgoing longwave radiation are found to be 3-times as likely during the wet than the dry phases of the waves.

Key words – Radiation-based equations, Calibration, Reference evapotranspiration, Humid, Dehradun.

1. Introduction

The tropical Madden Julian oscillation (MJO, Madden and Julian, 1972) modulates break and active periods in global monsoon systems (Rajeevan *et al*., 2010; Misra *et al*., 2017; Pai *et al*., 2011; Grimm *et al*., 2021). Although the research community has not come to agreement on the mechanisms that dominate the MJO, it coexists with a broader population of convectively coupled equatorial waves that also modulate deep convection (Kiladis *et al*., 2009). The dominant westward-moving equatorial wave at subseasonal timescales is the equatorial Rossby wave. The most typical form of such waves is the meridional mode $n = 1$ wave, which in a resting basic state forms pairs of gyres roughly symmetrically across the equator. This wave disperses westward at long wavelengths and eastward at short wavelengths and it always propagates westward relative to

the mean zonal flow. These Rossby waves occasionally form a systematic interference pattern with the MJO (Roundy and Frank, 2004 a&b), wherein as the MJO convection evolves eastward, these Rossby waves tend to form near particular longitudes and return westward. The MJO convection excites Rossby waves that radiate into the middle latitudes, but that later break into the tropics of the east Pacific, where they introduce gyres into the tropics that can then move westward or eastward, depending on the mean background flow (Gloeckler and Roundy, 2013; MacRitchie and Roundy, 2016). These westward-moving gyres become equatorial Rossby waves. Wang and Xie (1996) showed that as the eastward-moving intraseasonal oscillation moves eastward over the west Pacific during northern summer, gyres form there that then move back westward and northward across southeastern Asia to India. That time of year, the gyres form almost exclusively in the Northern Hemisphere with little Southern Hemisphere reflection. These gyres further impact the evolution of subseasonal variability in rainfall in the South Asian monsoon system. Webster (2020, chapters 9-11) provides a thorough summary of the potential vorticity dynamics of Rossby wave breaking along exit regions of the subtropical jet stream and illustrates how the resulting disturbances move through the flow to impact monsoon systems. This paper isolates the leading Eigen modes of westward-moving Rossby waves in the tropics and highlights their associations with the evolution of tropical convection over the Indian Ocean and the Indian subcontinent, as well as their associations with extratropical Rossby waves.

2. Data and methods

NOAA interpolated outgoing longwave radiation (OLR) data from 1974-2016 are filtered in the wave number frequency domain a westward wave numbers 1-10 and periods of 15-100 days to extract signals best associated with equatorial Rossby waves (Wheeler and Kiladis, 1999). Data are averaged from 15° N to 15° S, ultimately resulting in dominance of signals that are symmetric across the equator. Data are arranged with time going down the vertical axis and longitude across the horizontal and the covariance matrix is found. The eigenvectors of this matrix are the associated empirical orthogonal functions (EOFs). The leading two modes are retained. Higher EOFs also describe patterns consistent with equatorial Rossby waves, but are not analyzed because they are smaller in zonal scale. In order to diagnose the preferred atmospheric circulation and convective patterns associated with these waves, winds and geopotential height data, have their longterm means and seasonal cycles removed (including the first 4 harmonics) and then these are regressed against the equatorial Rossby wave principal components using the

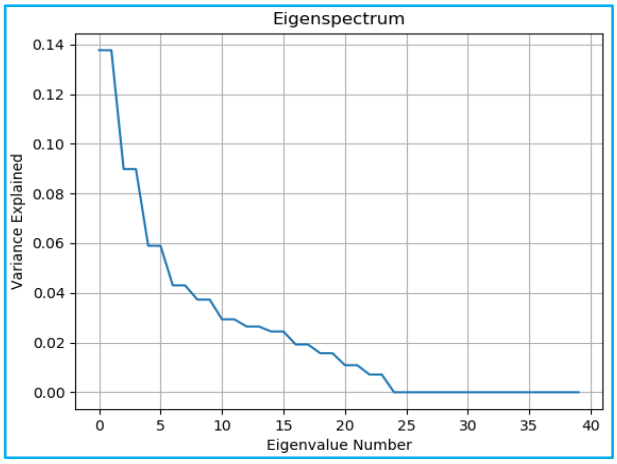

Fig. 1. First 40 Eigenvalues, standardized by the sum of Eigenvalues

method of seasonally varying regression slope coefficients of Roundy (2017) to diagnose the expectation value of anomalous patterns associated with the Rossby wave Principal Components that tend to occur as a function of day of the year. Eight phases of the index are isolated for convenience. In order to further assess the association of the phases of this index with convection in India, OLR anomalies are analyzed averaged over the region from 72.5° E to 85° E and from 12.5° N to 22.5° N. The period June-August is selected and days in which OLR index values are less than –1 standard deviation are counted during each equatorial Rossby wave phase when Rossby wave index amplitude is greater than 1 standard deviation. That number is then divided by the total number of days in that phase to give a percentage of days in the phase that are rendered convectively active. Statistical significance of regressed anomalies is done by a Monte Carlo experiment with 1000 repetitions resampling the original data included in the regressions. A similar resampling test, retaining all phase days, with replacement, is applied to assess the statistical stability of the analysis of active OLR days in each Rossby wave phase.

3. Results and discussion

Fig. 1 shows the Eigen spectrum of the equatorial Rossby wave filtered OLR anomalies, including the Eigen values divided by the sum of the Eigen values, showing only the first 40. The first two eigenvectors each explain 13.8% of the variance.

Figs. 2 and 3 show the first 2 EOF patterns and the second principal component (PC) lag regressed against the first. The EOFs are in quadrature in space, with EOF 2 situated 90° of phase west of EOF 1. The lag regression of PC 2 against PC 1 shows a global maximum at 5 days of lag, showing that, on average, PC2 maximizes 5 days after

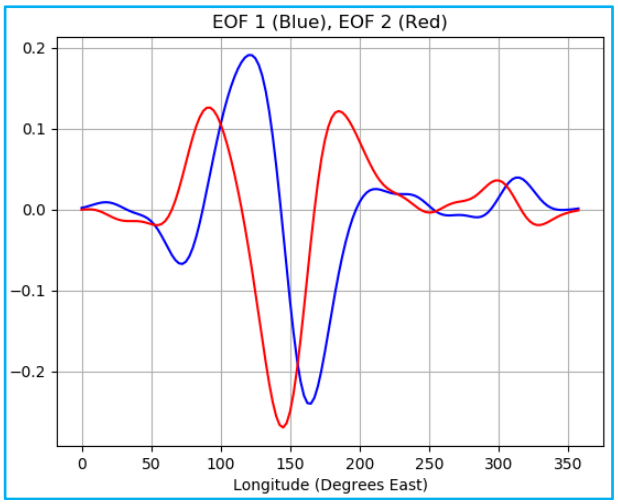

Fig. 2. Leading 2 Eigenvectors

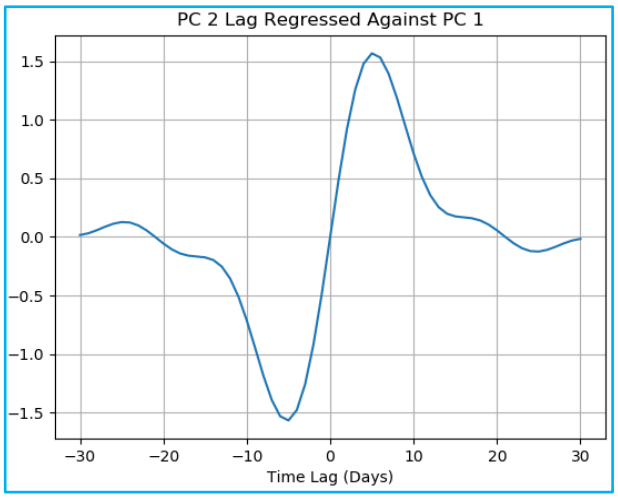

Fig. 3. Lag regression of PC 2 against PC 1, scaled to 2 standard deviations

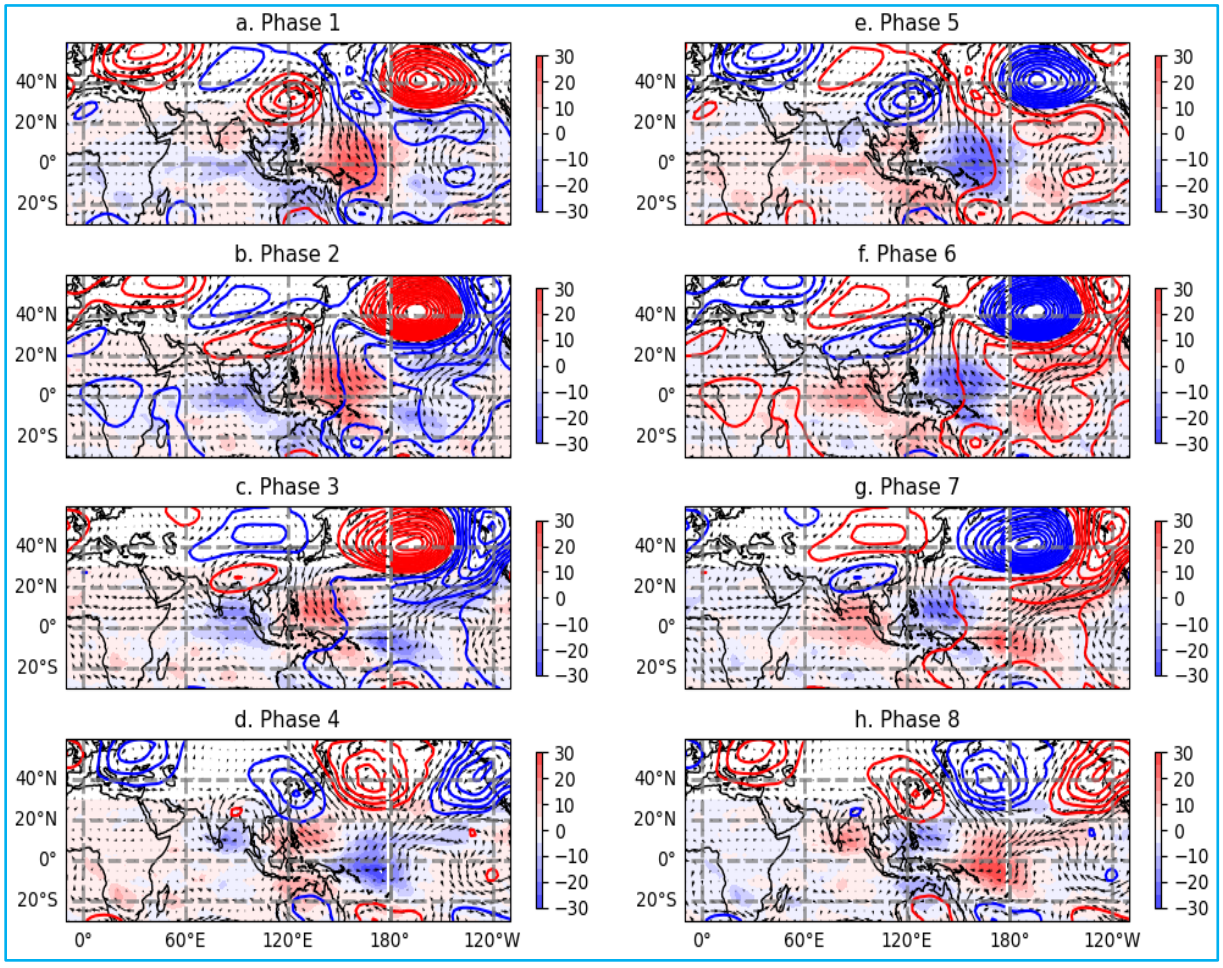

Figs. 4(a-h). Regressed OLR anomaly (shading, blue is negative and red positive, with contours every 10 Wm^{-2} and 200 hPa geopotential height (contours at 10 m interval with the zero line omitted) and wind anomalies (vectors). The method of seasonally varying regression slope coefficients is applied and results plotted for January 1. Height anomalies beyond roughly 2 contours are statistically significant at the 95% level based on a bootstrap resampling test

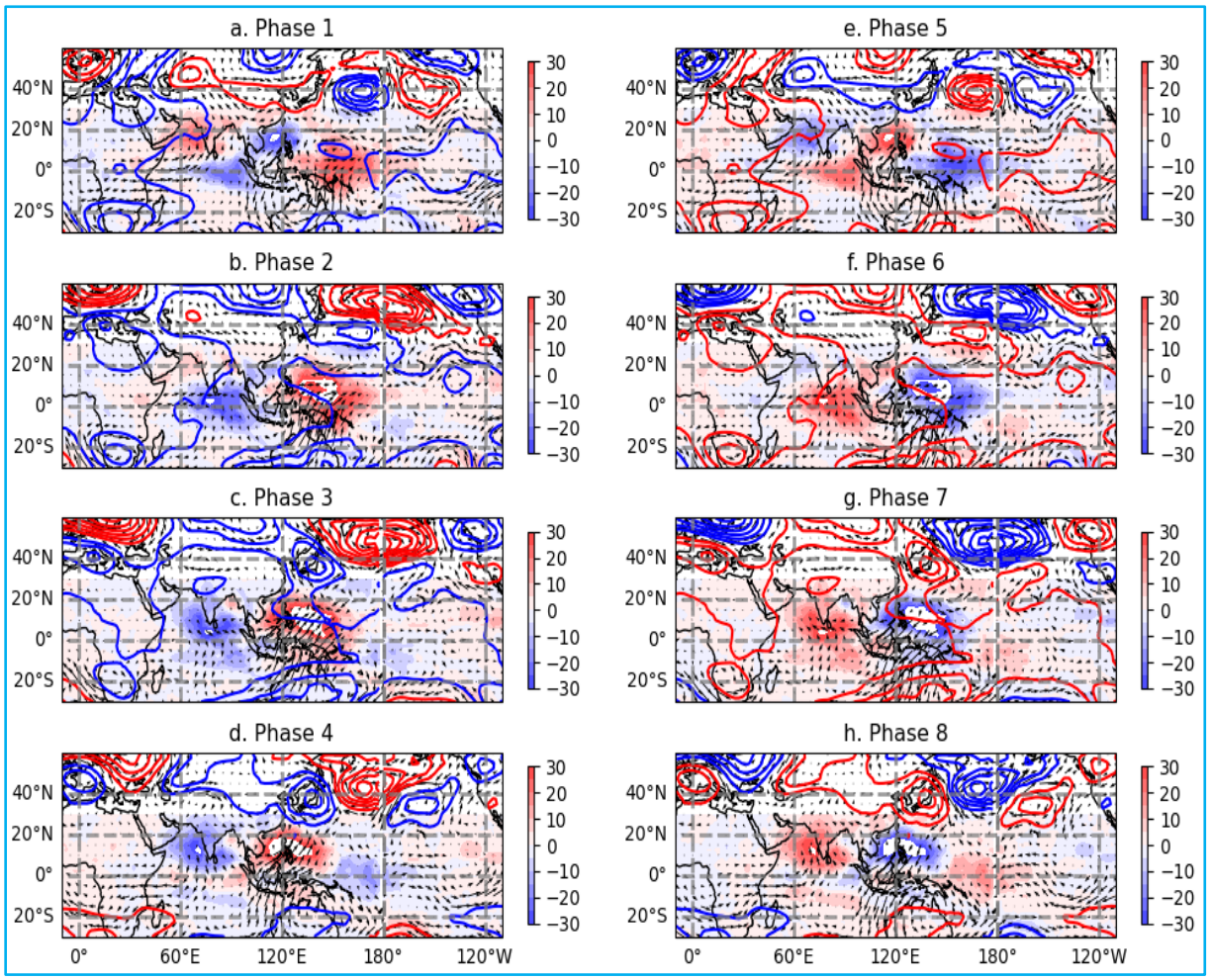

Figs. 5(a-h). Same as for Fig. 4, except with results plotted centered on July 1

PC1. Given a rough shift of 20° of longitude between the EOF patterns, this equates to a signal moving westward at roughly 5 ms^{-1}, which is in line with expectations for the equatorial Rossby wave (Kiladis *et al*., 2009).

Figs. 4(a-h) show tropical OLR and 200 hPa geopotential height anomalies for the eight selected phases of the leading ER band EOF pattern for January. Phase 1 shows a pair of negative OLR anomalies associated with enhanced convection centered around northern Australia and the Philippines and a negative anomalies also over the eastern equatorial Indian Ocean. A positive OLR anomaly is located over the western equatorial Pacific. As the phases progress, these anomalies move westward and the active convection suggested over the eastern Indian Ocean also moves northward toward southern India. Negative OLR anomalies appear on the equatorward sides of anticyclones and on the eastward equatorward sides of cyclones. High latitude North Pacific ridges occur when convection is located over the western tropical Pacific region, with the opposite during suppressed convection in the same region. Figs. 5(a-h) show the same regression of OLR anomalies, but for day of year 180, during the Northern Hemisphere summer. Although the Northern Hemisphere pattern shows substantial similarity to the northern winter result in Figs. 4(a-h), the Southern Hemisphere circulation pattern does not reflect any clear cross equatorial symmetry as appeared during southern summer. Convection originating on the equator during phase 1 evolves westward and northward through phase 5, after which it is replaced by a westward and northward-moving feature of suppressed convection. Although the geopotential height anomalies over the higher latitudes of the Pacific Ocean are weaker during northern summer, they appear in roughly the same positions relative to the tropical convective anomalies as they do during the winter.

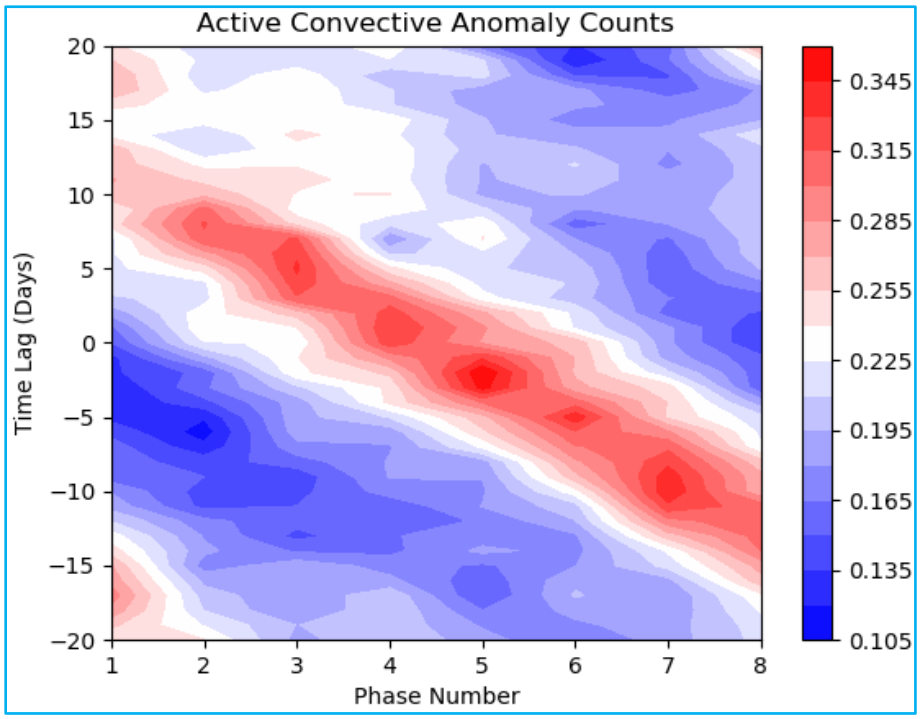

Fig. 6. Frequency of negative OLR anomalies in the region from 72.5° E to 85° E and 12.5° N to 22.5° N during each of the noted phases and at time lags there from

Fig. 6 shows how moist periods in the Indian monsoon, as traced by negative OLR anomalies, organize according to the phase of the ER wave index. Dry phases at lag = 0 are 1, 2, 7 and 8, while phases 4-6 tend to have more moist convection. The difference in moist convective days between the most moist and the least moist phases is greater than a factor of 3, showing that these waves have profound impact on the Indian monsoon.

4. Conclusions

An EOF analysis of OLR anomaly data filtered to extract signals associated with the equatorial Rossby wave yields an index pair associated with the largest spatial scale Rossby waves. Results show this leading principal component pair is associated with a Rossby wave pattern dominated by symmetry about the equator that moves westward at around 5 ms^{-1}. During the Northern Summer, the associated convective signals over the Indian Ocean region tend to originate near the equator in the eastern basin, after which they progress westward and northward across India. Similar to previous results, the Northern Summer signal is less associated with gyres in the Southern Hemisphere. During the Northern Winter, similar anomalies propagate mainly westward and show significant relationships with upper tropospheric circulation signals across the Northern Hemisphere extratropics, consistent with previous analysis that has shown that convection associated with these waves drives Rossby waves into the middle latitudes, which then move eastward on the background westerlies, until they again move equatorward and break in the Western Hemisphere. The breaking waves originate new equatorial Rossby wave signals that continue westward where they again modulate convection of the tropical warm pool regions. Analysis of OLR anomalies over a broad portion of India [Figs. 5(a-h)] suggest that the waves strongly modulate monsoon convective activity during June through August.

Acknowledgements

OLR data were provided by the NOAA Physical Sciences Laboratory. 200 hPa height and wind data were provided by the ERA5 reanalysis.

Disclaimer : The contents and views expressed in this study are the views of the authors and do not necessarily reflect the views of the organizations they belong to.

References

Gloeckler, L. C. and Roundy, P. E., 2013, "Modulation of the Extratropical Circulation by Combined Activity of the Madden-Julian Oscillation and Equatorial Rossby Waves during Boreal Winter", *Monthly Weather Review*, **141**, 4, 1347-1357. https://journals.ametsoc.org/view/journals/mwre/141/4/mwr-d-12-00179.1.xml.

Grimm, A. M., Hakoyama, L. R. and Scheibe, L. A., 2021, "Active and break phases of the South American summer monsoon: MJO influence and subseasonal prediction", *Clim. Dyn*., **56,** 3603-3624. https://doi.org/10.1007/s00382-021-05658-3.

Kiladis, G. N., Wheeler, M. C., Haertel, P. T., Straub, K. H. and Roundy, P. E., 2009, "Convectively coupled equatorial waves", *Rev. Geophys.*, **47**, RG2003. doi:10.1029/2008RG000266.

MacRitchie, K. and Roundy, P. E., 2016, "The two-way relationship between the Madden-Julian oscillation and anticyclonic wave breaking", *Q. J. R. Meteorol. Soc*., **142**, 2159-2167. https://doi.org/10.1002/qj.2809.

Madden, Roland A. and Paul R. Julian, 1972, "Description of global-scale circulation cells in the tropics with a 40-50 day period", *Journal of Atmospheric Sciences*, **29**, 6, 1109-1123.

Mishra, S. K., Sahany, S. and Salunke, P., 2017, "Linkages between MJO and summer monsoon rainfall over India and surrounding region", *Meteorol. Atmos. Phys.*, **129**, 283-296. https://doi.org/10.1007/s00703-016-0470-0.

Pai, D. S., Bhate, J., Sreejith, O. P. and Hatwar, H. R., 2011, "Impact of MJO on the intraseasonal variation of summer monsoon rainfall over India", *Clim. Dyn*., **36,** 41-55. https://doi.org/10.1007/s00382-009-0634-4.

Rajeevan, M., Gadgil, S. and Bhate, J., 2010, "Active and break spells of the Indian summer monsoon", *J. Earth Syst. Sci*., **119**, 229-247. https://doi.org/10.1007/s12040-010-0019-4.

Roundy, P. E. and Frank, W. M., 2004a, "Applications of a Multiple Linear Regression Model to the Analysis of Relationships between Eastward and Westward-Moving Intraseasonal Modes", *Journal of the Atmospheric Sciences*, **61**, 24, 3041-3048.https://doi.org/10.1175/JAS-3349.1.

Roundy, P. E. and Frank, W. M., 2004b, "Effects of Low-Frequency Wave Interactions on Intraseasonal Oscillations", *Journal of the Atmospheric Sciences*, **61**, 24, 3025-3040.

Roundy, P. E., 2017, "Diagnosis of seasonally varying regression slope coefficients and application to the MJO", *Q. J. R. Meteorol. Soc*., **143**, 1946-1952. https://doi.org/10.1002/qj.3054.

Wang, B. and Xie, Xiaosu, 1996, "A model of the Boreal Summer Intraseasonal Oscillation", *J. Atmos. Sci*., **54**, 72-86. https://doi.org/10.1175/1520-0469(1997)054<0072: AMFTBS> 2.0.CO;2.

Webster, P. J., 2020, "Dynamics of the Tropical Atmosphere and Oceans; Advancing Weather and Climate Science", John Wiley &U Sons. ISBN 0470662565. p536.